



**HAL**  
open science

# Sustainable and Efficient Low-Energy Light Emitters: A Series of One-Dimensional d 10 Coinage Metal–Organic Chalcogenolates, $[M(\text{o-SPhCO}_2\text{H})]_n$

Oleksandra Veselska, Nathalie Guillou, Maria Diaz-lopez, Pierre Bordet, Gilles Ledoux, Sébastien Lebègue, Adel Mesbah, Alexandra Fateeva, Aude Demessence

## ► To cite this version:

Oleksandra Veselska, Nathalie Guillou, Maria Diaz-lopez, Pierre Bordet, Gilles Ledoux, et al.. Sustainable and Efficient Low-Energy Light Emitters: A Series of One-Dimensional d 10 Coinage Metal–Organic Chalcogenolates,  $[M(\text{o-SPhCO}_2\text{H})]_n$ . ChemPhotoChem, 2022, 6 (5), pp.e202200030. 10.1002/cptc.202200030 . hal-03614640

**HAL Id: hal-03614640**

**<https://hal.science/hal-03614640>**

Submitted on 20 Sep 2022

**HAL** is a multi-disciplinary open access archive for the deposit and dissemination of scientific research documents, whether they are published or not. The documents may come from teaching and research institutions in France or abroad, or from public or private research centers.

L'archive ouverte pluridisciplinaire **HAL**, est destinée au dépôt et à la diffusion de documents scientifiques de niveau recherche, publiés ou non, émanant des établissements d'enseignement et de recherche français ou étrangers, des laboratoires publics ou privés.

Copyright

# Sustainable and Efficient Low-Energy Light Emitters: A Series of One-Dimensional d<sup>10</sup> Coinage Metal–Organic Chalcogenolates, [M(o-SPhCO<sub>2</sub>H)]<sub>n</sub>

Oleksandra Veselska,<sup>[a, b]</sup> Nathalie Guillou,<sup>[c]</sup> Maria Diaz-Lopez,<sup>[d]</sup> Pierre Bordet,<sup>[e]</sup> Gilles Ledoux,<sup>[f]</sup> Sébastien Lebègue,<sup>[g]</sup> Adel Mesbah,<sup>[a]</sup> Alexandra Fateeva,<sup>[h]</sup> and Aude Demessence<sup>\*[a, i]</sup>

A series of d<sup>10</sup> coinage metal thiosalicylate coordination polymers (CPs) is reported. The 1D structures of the three CPs are formed by M<sub>3</sub>S<sub>3</sub> fused hexagons for Cu and Ag compounds and interpenetrated helical chains for Au CP. Depending on the

metal, solid-state red and NIR emissive CPs are obtained with quantum yields up to 50%, providing a great opportunity to replace the actual emissive critical raw materials.

## Introduction

Today, the new generation of lighting displays requires new materials that exhibit bright emission, large color range emission, good stability, economic affordability and sustainability. In terms of stability, luminescent inorganic compounds are the best candidates. Unfortunately, their components, e.g. rare earth metals or cadmium in quantum dots, should be banned because of their toxicity and economic issues. Luminescent coordination polymers (CPs) that combine in the same material a ligand and a metal center present an alternative for lighting displays.<sup>[1]</sup> Among them, d<sup>10</sup> coinage metal-based CPs can be highly emissive and display good stability and affordability.<sup>[2]</sup> Indeed, these d<sup>10</sup> coinage metals are known for their bright photoemission, large range of emission energy, different photoluminescent processes, including thermally activated delayed fluorescence, aggregation-induced emission, which make them good candidates for

sustainable and efficient lighting.<sup>[3,2a]</sup> Numerous luminescent d<sup>10</sup> coinage metal clusters, complexes and CPs have been reported with different ligands.<sup>[2a,4]</sup> Nevertheless, neutral d<sup>10</sup> coinage metal–organic chalcogenolates (MOCs) are underreported due to their challenging structural characterization. Indeed, the high affinity between d<sup>10</sup> coinage metals and chalcogenol molecules implies fast reactivity, leading to formation of insoluble and poorly crystallized precipitates.<sup>[5]</sup> Still, the strong bond between the soft metal and soft chalcogenolate gives solids of high thermal and chemical stability.<sup>[2b,6]</sup>

Earlier, a new family of *para*-substituted compounds, [M(*p*-SPhCO<sub>2</sub>R)]<sub>n</sub>, with M = Cu, Ag, Au and R = H, Me, was synthesized and characterized by our group.<sup>[7]</sup> They form extended 2D M(I)–S networks and show interesting photophysical properties. For example, [Au(*p*-SPhCO<sub>2</sub>Me)]<sub>n</sub> CP has a bright yellow emission with a quantum yield (QY) as high as 70% in solid state at room temperature,<sup>[7a]</sup> while some other compounds of this family have multiple emission peaks which evolve independ-

[a] Dr. O. Veselska, Dr. A. Mesbah, Dr. A. Demessence  
Univ Lyon, Université Claude Bernard Lyon 1  
CNRS, UMR 5256  
Institut de Recherches sur la Catalyse et L'Environnement de Lyon  
(IRCELYON), Villeurbanne (France)  
E-mail: aude.demessence@ircelyon.univ-lyon1.fr

[b] Dr. O. Veselska  
Institute of Experimental and Applied Physics  
Czech Technical University in Prague  
Prague (Czech Republic)

[c] Dr. N. Guillou  
Institut Lavoisier de Versailles (ILV)  
UVSQ, Université Paris-Saclay  
CNRS, UMR 8180  
Versailles (France)

[d] Dr. M. Diaz-Lopez  
ISIS Facility, STFC Rutherford Appleton Laboratory and Diamond Light  
Source Ltd, Diamond House, Harwell Science and Innovation Campus,  
Didcot OX11 0DE (UK)


[e] Dr. P. Bordet  
Univ. Grenoble Alpes, CNRS  
Institut Néel, Grenoble (France)

[f] Dr. G. Ledoux  
Univ Lyon, Université Claude Bernard Lyon 1  
CNRS, UMR 5306  
Institut Lumière Matière (ILM)  
Villeurbanne (France)

[g] Dr. S. Lebègue  
Université de Lorraine, CNRS, UMR 7019  
Laboratoire de Physique et Chimie Théoriques (LPCT)  
Vandœuvre-lès-Nancy (France)

[h] Dr. A. Fateeva  
Univ Lyon, Université Claude Bernard Lyon 1  
CNRS, UMR 5615  
Laboratoire des Multimatériaux et Interfaces (LMI)  
Villeurbanne (France)

[i] Dr. A. Demessence  
BCMaterials (Basque Center for Materials  
Applications & Nanostructures)  
Universidad del País Vasco/Euskal Herriko Unibertsitatea UPV/EHU  
Leioa (Spain)

 Supporting information for this article is available on the WWW under  
<https://doi.org/10.1002/cptc.202200030>

ently with temperature, resulting in thermoluminescence.<sup>[7b-e]</sup>

Recently, a gold-based *meta*-substituted CP, [Au(*m*-SPhCO<sub>2</sub>H)]<sub>n</sub>, was reported as well. It has also a 2D Au(I)-S network associated with a yellow emission and a QY of 19% in solid state at room temperature. It was mixed with organic polymers to generate transparent and flexible luminescent thin films.<sup>[8]</sup>

To fully understand the network building, the photophysical properties of MOCs and their structure-properties relationship, a new series of isomeric CPs was investigated. For this goal, the *ortho*-mercaptobenzoic acid (*o*-HSPHCO<sub>2</sub>H), or thiosalicylic acid, has been used. It allowed to evaluate how altering the substituent position influences the M(I)-S network formation and the associated photophysical properties.

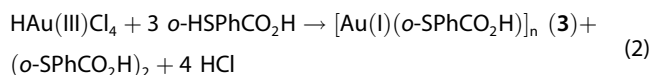
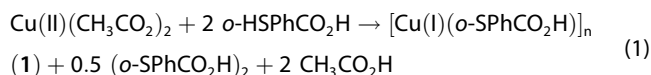
Interestingly, two compounds, thiosalicylates of Au(I)<sup>[9]</sup> and Ag(I),<sup>[10]</sup> have been already reported. The former showed red emission at room temperature, while the latter was reported to possess antimicrobial activity. Both presumably have polymeric nature, but their structures had not been solved.

Here, three new CPs based on the thiosalicylate ligand have been obtained and structurally characterized as [M(*o*-SPhCO<sub>2</sub>H)]<sub>n</sub> with M(I)=Cu (1), Ag (2) and Au (3). They form 1D structures and exhibit bright photoemission.

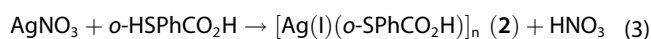
## Results and Discussion

### Syntheses

Highly crystalline powders of compounds 1 and 2 were synthesized using solvothermal conditions similarly to some previously reported coinage metals' thiolates.<sup>[11]</sup> For compound 3, the use of solvothermal conditions did not improve crystallinity, so synthesis at room temperature was performed. In the case of 1 and 3, an excess of thiosalicylic acid was used in order to reduce Cu(II) and Au(III) precursors, a process coupled with the oxidation of the ligand to the corresponding disulfide. The obtained powders were washed with ethanol to remove the excess of ligand and its oxidized form produced during the reaction as described in Equations (1) and (2):



Meanwhile, the synthesis of Ag(I)-based compound is a simple reaction of coordination of the organic ligand by the metal cation from the Ag(I) precursor, as shown in Equation (3):



### Structural determinations

For all the three compounds, high resolution Powder X-Ray Diffraction (PXRD) data were collected at the beamline ID15A of European Synchrotron Radiation Facility (ESRF, Grenoble, France; Figure 1).

These three compounds crystallize in the tetragonal *P*4<sub>2</sub>/*n* space group (Table S1, Supporting Information).<sup>[12]</sup> Compounds 1 and 2 are isostructural and closely related to previously reported [Cu(SR)]<sub>n</sub> forming 1D columns, e.g. [Cu(SMe)]<sub>n</sub>,<sup>[13]</sup> [Cu(SPh)]<sub>n</sub>,<sup>[14]</sup> [Cu(*p*-SPhMe)]<sub>n</sub>,<sup>[14]</sup> [Cu(*p*-SPhOMe)]<sub>n</sub>,<sup>[14]</sup> (Figure 2(a), (b)). The columns are made of six-membered ring of M<sub>3</sub>S<sub>3</sub> facing each other through an inversion center, connected through trigonal coinage metal atoms and μ<sub>3</sub> bridging thiolates.

For compound 1, Cu–S distances and angles are summarized and compared with those of [Cu(SPh)]<sub>n</sub> in Table S2, showing close resemblance between the two structures. The neighboring CP columns are connected through dimeric hydrogen bonds between the carboxylic acid groups (Figure 2(c)).

Concerning compound 2 (Table S1, Figure S1, Supporting Information), it is important to note that this type of 1D columnar Ag(I)-S network is observed for the first time for Ag(I)-based chalcogenolate. The Ag(I)-S distances and angles are summarized in Table S2.

Similar fused hexagons, M<sub>3</sub>S<sub>3</sub>, are observed in both 1D and 2D CPs. For example, in [Cu(*p*-SPhCO<sub>2</sub>Me)]<sub>n</sub> or [Cu(*p*-SPhOH)]<sub>n</sub>, M<sub>3</sub>S<sub>3</sub> rings are arranged into infinite undulated 2D-networks. They are present in slightly distorted version, in [Cu(*p*-SPhCO<sub>2</sub>H)]<sub>n</sub>,<sup>[7d]</sup> and [Ag(*p*-SPhCO<sub>2</sub>R)]<sub>n</sub> (R=H, Me)<sup>[7e]</sup> as well. But in [M(*o*-SPhCO<sub>2</sub>H)]<sub>n</sub>, M=Cu, Ag, the steric hindrance of the carboxylic acid positioned close to the coordination site prevents the propagation of arranged M<sub>3</sub>S<sub>3</sub> hexagons into a 2D-network, giving rise to the bent arrangement forming a 1D column (Figure S3, Supporting Information).

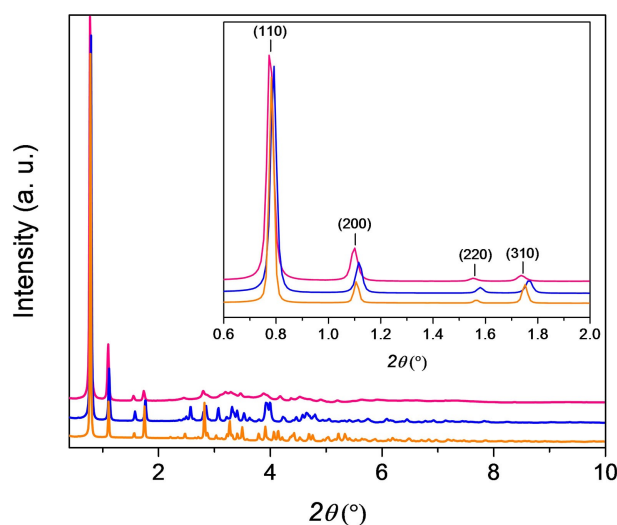
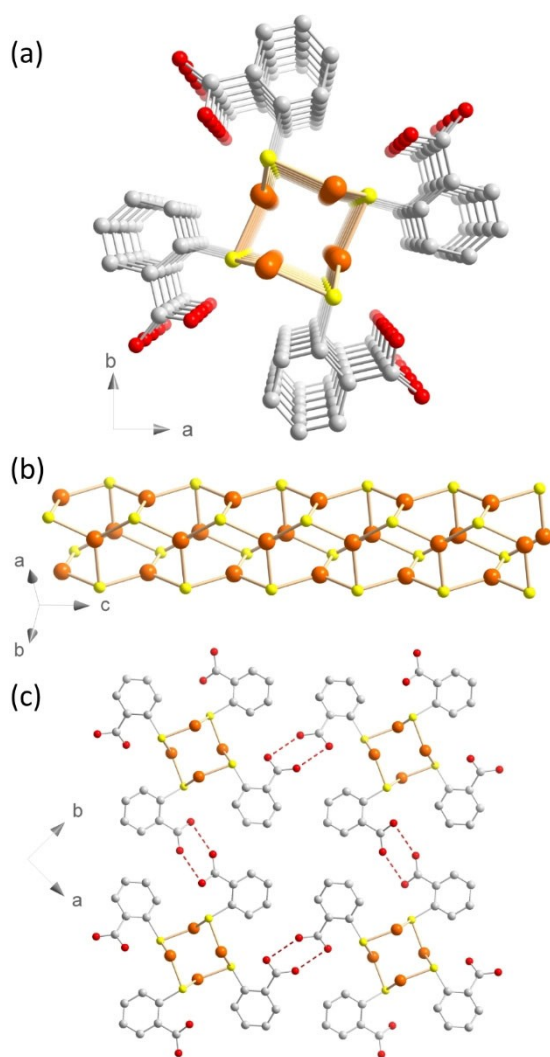


Figure 1. Experimental PXRD patterns of 1 (orange), 2 (blue) and 3 (pink) ( $\lambda = 0.17965 \text{ \AA}$ ). A zoom is shown as inset.



**Figure 2.** Structure of  $[\text{Cu}(\text{o-SPhCO}_2\text{H})]_n$  1: (a) central projection along the  $c$  axis; (b) view of the Cu–S arrangement; (c) view along the  $c$  axis with red dotted lines representing the hydrogen bonds network. Orange, Cu; yellow, S; red, O; grey, C. Hydrogen atoms are omitted for clarity.

The poor crystallinity of **3** precluded an in-depth structural investigation using solely PXRD and only limited information could be extracted for this compound. However, the close positions of the first four most intense peaks (corresponding to (1 1 0), (2 0 0), (2 2 0) and (3 1 0) reflections) of these three CPs and the similar PXRD patterns, point out their structural proximity (Figure 1, inset). Therefore, a pair distribution function (PDF) study was performed to gain deeper insight into structure of **3**. PDF represents a distribution of interatomic distances in a given sample. Indeed, it allows to get quantitative information on the local atomic arrangement and structural coherence length independently of the crystalline state of the material and was shown to provide important structural information for complex compounds such as amorphous inorganic zeolites,<sup>[15]</sup> MOFs and CPs.<sup>[16]</sup>

The comparison of the PDFs of **2** and **3** confirms the similarities of the structures<sup>[17]</sup> (Figure S4(a), (b), Supporting Information). Indeed, the positions of the first peaks at 3.4, 4.6,

5.6 and 6.9 Å for **2** and at 3.5, 4.6, 5.8 and 7.3 Å for **3** are close and this is also true for the peaks at larger distances. The amplitude of oscillations for **3** is strongly damped at longer distances due to the decrease of the structural coherence length. This is observed for broad features centered at 17 Å, 30 Å, 43 Å, 58 Å and 70 Å corresponding to the distances between first-, second- and following neighboring  $[\text{MS}]_n$  columns (Figure S4(b), Supporting Information)). Thus, the structure of **2** (Figure S5, Supporting Information) can be used as a starting model for the Rietveld refinement of the structural model of **3**, with silver atoms being replaced by gold atoms. Although some discrepancies in the Rietveld plot can be observed (Table S1, Figure S6, Supporting Information), the lowering of the symmetry did not improve the agreement between observed and calculated patterns. Thus, the obtained structural model, in the  $P4_2/n$  space group symmetry, was then used for the PDF refinement. During the refinement in MolPDF software,<sup>[18]</sup> the organic ligand was included in the structural model being fully constrained (i.e. considered as a rigid block molecule). Few information about the position of the phenyl ring compared to the Au(I)–S chains can be obtained with this method, because of the large difference in the atomic numbers between gold and sulfur atoms in comparison to carbon, oxygen and hydrogen. Refinement gives a good fit to the data in the range from 2 Å to 25 Å (Figure 3). The M(I)–S network of **3** is organized differently in comparison to **2**, with Au(I) atom coordinated to two sulfur atoms and thiolates bridging two gold atoms (Figure 4). This coordination mode is in agreement with the common linear two-coordinated gold atom environment and leads to the formation of a double interpenetrated helical chain similar to  $[\text{Au}(\text{SPh})]_n$ .<sup>[11]</sup> The intrachain contacts between neighboring gold atoms are of 3.44(2) Å, while interchain contacts are of 3.64(2) Å (Figure 4(b)). The comparison of the PDF of **3** and the previously reported  $[\text{Au}(\text{SPh})]_n$  confirms that Au–S arrangement is similar in these compounds (Table S2, Figure S7, Supporting Information).

The S K-edge XANES and EXAFS data were collected as well (Figure S8, Supporting Information). The EXAFS data were fitted

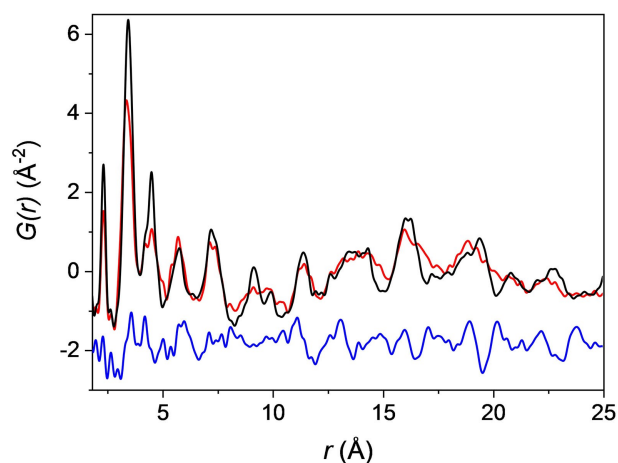


**Figure 3.** PDF refinement of **3** showing observed (red line), calculated (black line), and difference (blue line) curves.

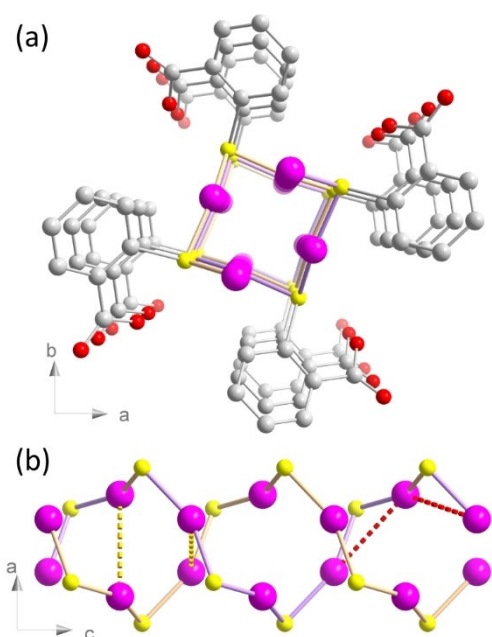


**Figure 4.** Structure representations of  $[\text{Au}(o\text{-SPhCO}_2\text{H})]_n$ , **3**: (a) central projection along the  $c$  axis; (b) view of the Au–S arrangement along  $b$  axis; Au–S–Au helical chains are represented in beige and purple colors. Pink, Au; yellow, S; red, O; grey, C. Hydrogen atoms are omitted for clarity. Red and yellow dotted lines represent intra- and interchain Au(I)–Au(I) contacts.

using the average models determined from PXRD data (Table S3, Figure S8(b), Supporting Information). The refinements show good agreement with the experimental data confirming the adequacy of proposed structural models.

### Additional characterizations

From SEM images, the 1D crystalline structures adopt 1D shape crystallites (Figure S9, Supporting Information): **1** is composed of long needles with wide length distribution ( $\approx 1\text{--}20\ \mu\text{m}$ ), **2** is constituted of stacked wires of about 90 nm in diameter and 1  $\mu\text{m}$  in length and **3** is composed of long micrometer-scale fibers of 250 nm in diameter.

FTIR spectroscopy (Figure S10, Supporting Information) shows the existence of broad  $\nu(\text{OH})$  bands around  $3000$  and  $2600\ \text{cm}^{-1}$  for the three CPs. They are consistent with the presence of hydrogen bonds between the carboxylic acid functions. The antisymmetric vibration of the carboxylic acid group is observed at  $1680\ \text{cm}^{-1}$ . It is close to the band of free-standing ligand and is in good agreement with non-coordinated acid groups. A relatively broad band of out of plane vibration of OC–OH is observed at  $905\ \text{cm}^{-1}$ .<sup>[19]</sup>

The thermo-gravimetric and elemental analyses of the three CPs confirm the purity of the compounds with an expected metal and organic content (Figure S11, Supporting Information). All compounds show relatively good thermal stability under air, with decomposition temperatures starting at  $200^\circ\text{C}$ ,  $260^\circ\text{C}$  and  $270^\circ\text{C}$  for Cu(I)-, Ag(I)- and Au(I)-based CPs, respectively. The thermal stability of **3** is higher than for

$[\text{Au}(\text{SPh})]_n$  ( $270^\circ\text{C}$  vs.  $200^\circ\text{C}$ ). It may be due to the presence of hydrogen bonding which reinforces the structure.<sup>[11]</sup>

### Photophysical characterizations

Compounds **1** and **3** under natural light are pale yellow and pale beige powders, respectively, while compound **2** is an orange powder (Figure 5(a)). Compounds **1** and **3** exhibit high-energy absorption between  $\lambda_{\text{abs}} = 300\text{--}350\ \text{nm}$ , which is assigned to  $\pi\text{-}\pi^*$  transitions of the phenyl group of the ligand (Figure S12(a), Supporting Information).<sup>[20]</sup> Compound **1** has also a low intensity shoulder between  $400\text{--}450\ \text{nm}$ . It presumably results from MLCT (Metal-to-Ligand Charge Transfer) or LMCT (Ligand-to-Metal Charge Transfer) transition modified by  $\text{M}\cdots\text{M}$  contacts.<sup>[21]</sup> This profile is similar to the isostructural  $[\text{Cu}(\text{SPh})]_n$ .<sup>[14]</sup> Compound **2** shows a broad unstructured band between  $\lambda_{\text{abs}} = 300\text{--}450\ \text{nm}$ , presumably as a result of an electronic transition from the  $\sigma(\text{Ag}\text{--}\text{S})$  orbital to an empty  $\pi^*$  antibonding orbital located at the phenyl group of the ligand.<sup>[22]</sup>

The optical band gaps are 2.43, 2.23 and 2.83 eV for **1**, **2** and **3**, respectively (Figure S12(b), Supporting Information). The band gap of **1** is comparable to other reported copper(I)-based 1D-MOCs (2.23–2.68 eV),<sup>[14]</sup> and the value of **3** is fairly close to the one of  $[\text{Au}(\text{SPh})]_n$  (2.8 eV).<sup>[11]</sup>

The excitation of **2** under a UV light in solid state at room temperature (RT) results in an intense orange emission, while **1** and **3** show weak dark red emissions (Figure 5(a)). The emission spectra at RT have broad featureless profiles centered at 700, 634 and 787 nm for **1**, **2** and **3**, respectively (Table 1). The order of the positions of these emission maxima from Ag, Cu and Au follows the one observed for a series of isostructural  $d^{10}$  coinage metal complexes.<sup>[23]</sup> Maxima of the excitation are centered at 412, 480 and 376 nm from **1** to **3** (Figure 5(b), S13, see the Supporting Information, and Table 1). The large Stokes shifts of  $9988\ \text{cm}^{-1}$ ,  $5060\ \text{cm}^{-1}$  and  $13886\ \text{cm}^{-1}$  point out highly distorted excited states. The QYs are of 0.2% (**1**), 51.6% (**2**) and

**Table 1.** Photophysical properties of **1**, **2** and **3**. HT is for high temperature.

| Compound  | <b>1</b>  | <b>2</b>   | <b>3</b>                              |
|---|---|--|---------------------------------------|
| $(\lambda_{\text{exc}}, \lambda_{\text{em}})$ at 93 K [nm]  | (412, 719)  | (476, 654)   | (368, 813)                            |
| $(\lambda_{\text{exc}}, \lambda_{\text{em}})$ at 293 K [nm] | (412, 700)  | (480, 634)   | (376, 787)                            |
| $(\lambda_{\text{exc}}, \lambda_{\text{em}})$ at HT [nm]    | (412, 697) at 413 K                               | (484, 627) at 443 K                                | (376, 756) at 473 K                   |
| Stokes shift at 93 K [ $\text{cm}^{-1}$ ]                   | 10364   | 5718   | 14874                                 |
| Stokes shift at 293 K [ $\text{cm}^{-1}$ ]                  | 9986  | 5060   | 13889                                 |
| Stokes shift at HT [ $\text{cm}^{-1}$ ]                     | 9925  | 4712   | 13368                                 |
| QY at 293 K, %  | 0.2   | 51.6   | 7.3                                   |
| Lifetime decay at 93 K                                      | 0.8 $\mu\text{s}$ (46%)<br>36 $\mu\text{s}$ (54%) | 37 $\mu\text{s}$ (100%)                            | 5.5 $\mu\text{s}$ (100%)              |
| Lifetime decay at 293 K                                     | 7 ns (98%)<br>4.4 $\mu\text{s}$ (2%)              | 0.8 $\mu\text{s}$ (70%)<br>163 $\mu\text{s}$ (30%) | 1.4 $\mu\text{s}$ (100%)              |
| Lifetime decay at HT  | 2 ns (98%)<br>1 $\mu\text{s}$ (2%)                | 7 ns (11%)<br>156 $\mu\text{s}$ (89%)              | 84 ns (98%)<br>1.4 $\mu\text{s}$ (2%) |

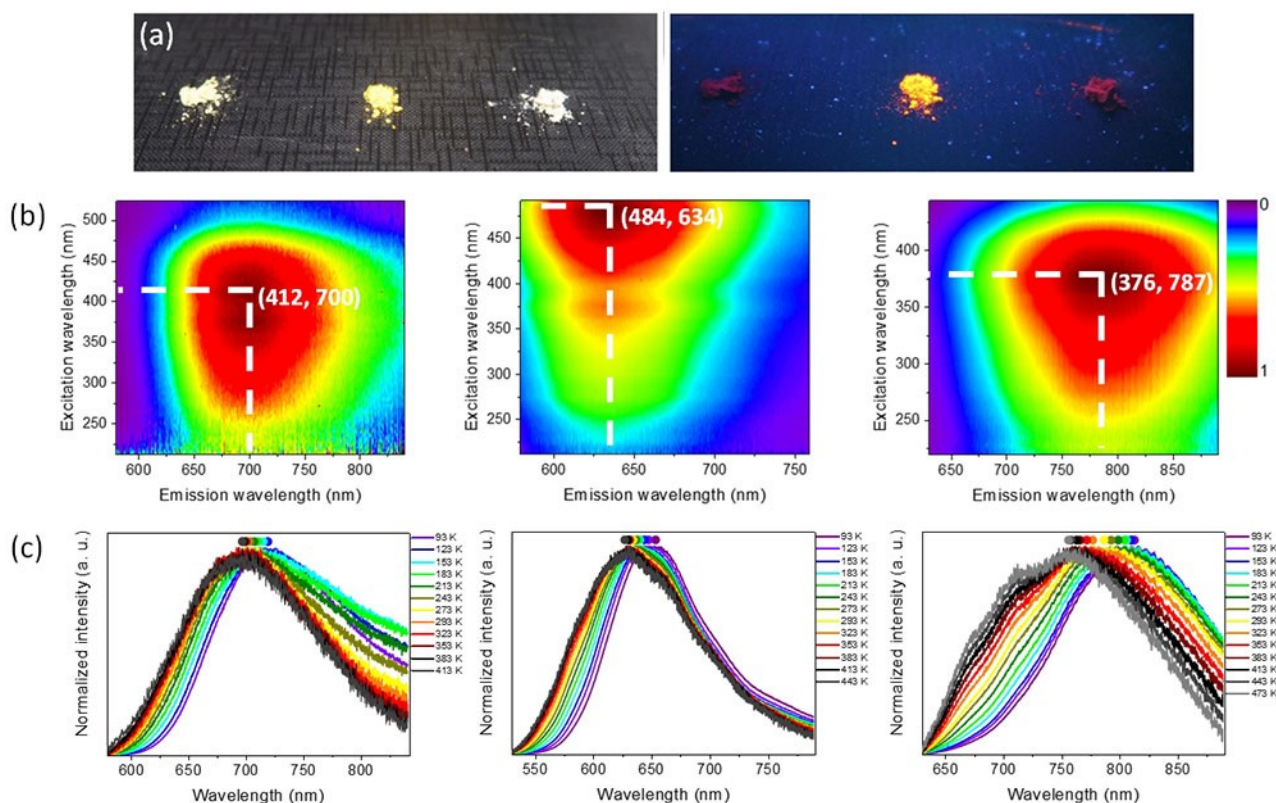


**Figure 5.** (a) Photographs of **1**, **2** and **3** under ambient light (left) and UV lamp (right) in solid state at room temperature. (b) From the left to the right: 2D maps of the emission and excitation spectra of the compounds **1**, **2** and **3**, respectively, carried out in the solid state at 293 K. (c) From the left to the right: normalized emission spectra of the compounds **1** ( $\lambda_{\text{exc}} = 412$  nm), **2** ( $\lambda_{\text{exc}} = 484$  nm) and **3** ( $\lambda_{\text{exc}} = 376$  nm), respectively, carried out in the solid state at variable temperatures; filled colored circles above the spectra indicate the position of peak maximum at corresponding temperature.

7.3% (**3**) at RT in solid state (Table 1). The important QY of the orange emissive Ag-based CP offers a great opportunity for full-color display. The near infrared (NIR) emission of **3** has the highest QY reported for Au-based NIR-emitters<sup>[24]</sup> providing good potential for bioimaging with non-toxic metal.

Upon heating, the CPs preserve emission and their maxima is blue shifted to 697 nm at 413 K for **1**, 627 nm at 443 K for **2** and 756 nm at 473 K for **3** (Table 1). This demonstrates their good photoluminescent efficiency even at high temperature. Upon cooling to 93 K, all compounds show a bathochromic shift of the emission (Figure 5(c)). Thus, the emission maxima for **1** to **3** are at 719 nm ( $\Delta_{413-93\text{K}} = 22$  nm,  $439\text{ cm}^{-1}$ ,  $0.054$  eV), 654 nm ( $\Delta_{443-93\text{K}} = 27$  nm,  $658\text{ cm}^{-1}$ ,  $0.082$  eV) and 813 nm ( $\Delta_{473-93\text{K}} = 57$  nm,  $928\text{ cm}^{-1}$ ,  $0.115$  eV), respectively (Table 1).

Compounds **1** and **2** display two lifetime components at RT: 7 ns (98%), 4.4  $\mu\text{s}$  (2%) and 0.8  $\mu\text{s}$  (70%), 163  $\mu\text{s}$  (30%), respectively, whereas **3** has a monoexponential lifetime decay of 1.4  $\mu\text{s}$  (Figures S14–S19, Tables 1 and S4–S6). Upon cooling to 93 K, the lifetime decays turn to be longer reaching 0.8  $\mu\text{s}$  and 36  $\mu\text{s}$  for **1**, 37  $\mu\text{s}$  for **2**, and 5.5  $\mu\text{s}$  for **3** due to the increase in rigidity, also indicating a decrease of the non-radiative rate constant (Table 1 and Figure S20–22). The presence of two lifetimes is indicative of two thermally non-equilibrated states. The large Stokes shifts and long lifetime decays at low

temperature are typical of phosphorescent processes involving triplet states.

Density functional theory<sup>[25]</sup> calculations have been carried out for the three compounds to obtain the density of states (DOS) in order to assign the origin of the photoemission. Firstly, our calculated band gaps of **1** to **3** (2.28, 2.44 and 3.05 eV) are in good agreement with the measurements. Secondly, **1**, **2** and **3** have similar DOSs (Figure S23–24 and Figure 6): they show that the top of the valence bands is first mainly occupied by sulfur, then carbon and after the metals. The conduction bands derive mostly from the carbon atoms. This points out that the electronic density is mostly localized on the ligand, and that the process of light emission most probably originates from a Ligand-to-Metal Charge Transfer (LMCT).

These attributions are in good agreement with similar [Cu(SPh)]<sub>n</sub> and [Au(SPh)]<sub>n</sub> compounds, that are structurally similar to **1** and **3**, respectively, (Table S2, Figure S7) and have emission maxima located at 650 nm (RT, solid state)<sup>[11]</sup> and at 684 nm (RT, solid state),<sup>[26]</sup> respectively. The emission origin of [Cu(SPh)]<sub>n</sub> and [Au(SPh)]<sub>n</sub> has been attributed to LMCT and LMMCT transitions with MC contribution.<sup>[11,26]</sup>

Normally, the introduction of electron-withdrawing ( $-\text{CO}_2\text{H}$ ) group on the ligand is expected to blue shift the emission of **1** and **3** with respect to that of [Cu(SPh)]<sub>n</sub> and [Au(SPh)]<sub>n</sub> if

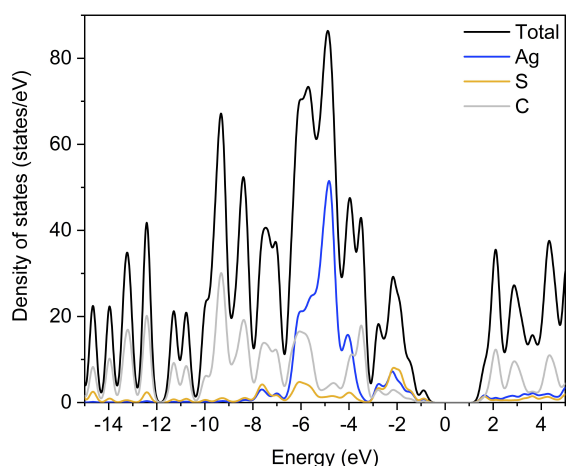


Figure 6. Computed density of states of 2.

LM(M)CT is involved in luminescence origin.<sup>[27]</sup> However, the opposite is observed. The emission is red shifted by  $1099\text{ cm}^{-1}$  for Cu(I)-based compounds and by  $1913\text{ cm}^{-1}$  for Au(I)-based compounds (at RT). On the other hand, an emission red shift can be induced by a decrease of the metal-metal distances in coinage metal-based compounds due to stronger metallophilic interactions.<sup>[27]</sup> This phenomenon is observed for the CPs when the temperature decreases meaning a shortening of the metallophilic bonds.<sup>[28]</sup> Nevertheless when comparing thiophenolates and the thiosalicylic acid derivatives, the metal-metal distances are slightly longer in the latter ones (Table S2). The observed red shift probably originates due to the conformational change/distortion of the coordination network<sup>[29]</sup> (see angles in Table S2) because of the presence of hydrogen bonds.

## Conclusion

In summary, a new family of closely related thiosalicylates of Cu(I) (1), Ag(I) (2) and Au(I) (3) CPs was prepared in one-pot syntheses and fully characterized. Structure resolutions from PXRD and PDF give access to the 1D structures formed by fused  $M_3S_3$  hexagons for 1 and 2 and interpenetrated  $M_2S_2$  chains in  $[Au(o\text{-SPhCO}_2\text{H})]_n$ . The three coinage-metal-based CPs exhibit photoluminescent properties originating from LMCT and with high QYs for the orange-emissive Ag(I)-CP (QY = 51.6%) and the NIR emitting Au(I)-based CPs (QY = 7.3%). The high QY of compound 2 makes it an attractive candidate material for sustainable and efficient illumination. It is also worth noting, that compound 3 represents interesting properties in comparison to other gold-based NIR-emitter CPs, which are normally known to be rare and have faint luminescence.<sup>[24]</sup> Thus, these new CPs underline that extended networks of coinage metal chalcogenolates can be potential candidates for low-energy emitting materials and a great solution to replace the critical lanthanide-based materials.

## Experimental Section

The supporting information contains syntheses, crystallographic data, PXRD, PDF, XANES, SEM, IR, TGA, UV-visible absorption, emission-excitation spectra and lifetime decays.

Deposition Number(s) <https://www.ccdc.cam.ac.uk/services/structures?id=doi:10.1002/cptc.202200030> 2051762 (for 1), 2051763 (for 2), 2051764 (for 3) contain(s) the supplementary crystallographic data for this paper. These data are provided free of charge by the joint Cambridge Crystallographic Data Centre and Fachinformationszentrum Karlsruhe <http://www.ccdc.cam.ac.uk/structuresAccessStructures> service.

## Acknowledgements

The authors acknowledge ESRF and Soleil Synchrotron for provision synchrotron radiation facilities at the beamline ID15A (proposal CH-5144) and LUCIA (proposal 20190354), respectively. Dr. Marco Di Michiel and Dr. Benedikt Lassalle are warmly acknowledged for their great help during the experiments at ESRF and Soleil synchrotrons, respectively. The CTU is thanked for providing the microscopy facilities. Dr. Katerina Dohnalova Newell from Institute of Physics, University of Amsterdam, is thanked for performing the quantum yield measurements. This work was supported by the French National Agency (MEMOL project ANR-16-JTIC-0004-01). OV thanks the Rhône-Alpes region for her PhD grant and European Regional Development Fund-Project for her actual position (No. CZ.02.1.01/0.0/0.0/16\_019/0000766). The European Commission is acknowledged by AD for the Marie Skłodowska-Curie Individual Fellowship (101031503 – AniMOC).

## Conflict of Interest

The authors declare no conflict of interest.

## Data Availability Statement

The data that support the findings of this study are available in the supplementary material of this article.

**Keywords:** coordination polymers · thiolate ligands · photoluminescence · NIR emission

- [1] a) M. Pan, W.-M. Liao, S.-Y. Yin, S.-S. Sun, C.-Y. Su, *Chem. Rev.* **2018**, *118*, 8889; b) Y. Cui, J. Zhang, H. He, G. Qian, *Chem. Soc. Rev.* **2018**, *47*, 5740; c) J. Heine, K. Müller-Buschbaum, *Chem. Soc. Rev.* **2013**, *42*, 9232.
- [2] a) V. W.-W. Yam, V. K.-M. Au, S. Y.-L. Leung, *Chem. Rev.* **2015**, *115*, 7589; b) S. Vaidya, O. Veselska, A. Zhadan, M. Daniel, G. Ledoux, A. Fateeva, T. Tsuruoka, A. Demessence, *J. Mater. Chem. C* **2020**, *8*, 8018.
- [3] a) P. Alam, C. Climent, P. Alemany, I. R. Laskar, *J. Photochem. Photobiol. C* **2019**, *41*, 100317; b) C.-W. Hsu, C.-C. Lin, M.-W. Chung, Y. Chi, G.-H. Lee, P.-T. Chou, C.-H. Chang, P.-Y. Chen, *J. Am. Chem. Soc.* **2011**, *133*, 12085.
- [4] M. J. Katz, K. Sakai, D. B. Leznoff, *Chem. Soc. Rev.* **2008**, *37*, 1884.
- [5] O. Veselska, A. Demessence, *Coord. Chem. Rev.* **2018**, *355*, 240.
- [6] a) S.-H. Cha, J.-U. Kim, K.-H. Kim, J.-C. Lee, *Chem. Mater.* **2007**, *19*, 6297; b) Y. X. Zhang, H. C. Zeng, *Adv. Mater.* **2009**, *21*, 4962.

- [7] a) C. Lavenn, N. Guillou, M. Monge, D. Podbevšek, G. Ledoux, A. Fateeva, A. Demessence, *Chem. Commun.* **2016**, 52, 9063; b) O. Veselska, L. Okhrimenko, N. Guillou, D. Podbevšek, G. Ledoux, C. Dujardin, M. Monge, D. M. Chevrier, R. Yang, P. Zhang, A. Fateeva, A. Demessence, *J. Mater. Chem. C* **2017**, 5, 9843; c) O. Veselska, D. Podbevšek, G. Ledoux, A. Fateeva, A. Demessence, *Chem. Commun.* **2017**, 53, 12225; d) O. Veselska, L. Cai, D. Podbevšek, G. Ledoux, N. Guillou, G. Pilet, A. Fateeva, A. Demessence, *Inorg. Chem.* **2018**, 57, 2736; e) O. Veselska, C. Dessal, S. Melizi, N. Guillou, D. Podbevšek, G. Ledoux, E. Elkaim, A. Fateeva, A. Demessence, *Inorg. Chem.* **2019**, 58, 99.
- [8] O. Veselska, N. Guillou, G. Ledoux, C.-C. Huang, K. Dohnalova Newell, E. Elkaim, A. Fateeva, A. Demessence, *Nanomaterials* **2019**, 9, 1408.
- [9] R. E. Bachman, S. A. Bodolosky-Bettis, *Z. Naturforsch.* **2009**, 64b, 1491.
- [10] K. Nomiyama, Y. Kondoh, K. Onoue, N. C. Kasuga, H. Nagano, M. Oda, T. Sudoh, S. Sakuma, *J. Inorg. Biochem.* **1995**, 58, 255.
- [11] C. Lavenn, L. Okhrimenko, N. Guillou, M. Monge, G. Ledoux, C. Dujardin, R. Chiriac, A. Fateeva, A. Demessence, *J. Mater. Chem. C* **2015**, 3, 4115.
- [12] *Deposition Numbers 2051762 (1) and 2051763 (2) contain the supplementary crystallographic data for this paper. These data are provided free of charge by the joint Cambridge Crystallographic Data Centre and Fachinformationszentrum Karlsruhe Access Structures service.*
- [13] M. Baumgartner, H. Schmalle, C. Baerlocher, *J. Solid State Chem.* **1993**, 107, 63.
- [14] C.-M. Che, C.-H. Li, S. S.-Y. Chui, V. A. L. Roy, K.-H. Low, *Chem. Eur. J.* **2008**, 14, 2965.
- [15] J. E. Readman, P. M. Forster, K. W. Chapman, P. J. Chupas, J. B. Parise, J. A. Hriljac, *Chem. Commun.* **2009**, 23, 3383.
- [16] a) T. D. Bennett, A. L. Goodwin, M. T. Dove, D. A. Keen, M. G. Tucker, E. R. Barney, A. K. Soper, E. G. Bithell, J.-C. Tan, A. K. Cheetham, *Phys. Rev. Lett.* **2010**, 104, 115503; b) S. Vaidya, O. Veselska, A. Zhadan, M. Diaz-Lopez, Y. Joly, P. Bordet, N. Guillou, C. Dujardin, G. Ledoux, F. Toche, R. Chiriac, A. Fateeva, S. Horike, A. Demessence, *Chem. Sci.* **2020**, 11, 6815.
- [17] C. A. Simpson, C. L. Farrow, P. Tian, S. J. L. Billinge, B. J. Huffman, K. M. Harkness, D. E. Cliffler, *Inorg. Chem.* **2010**, 49, 10858.
- [18] J. Rodriguez-Carvajal, A. Bytchkov, *Institut Laue-Langevin, Grenoble, France* **2016**.
- [19] E. Pretsch, P. Buhlmann, M. Badertscher, *Structure Determination of Organic Compounds*, 4 ed., Springer-Verlag Berlin Heidelberg, **2009**.
- [20] J. S. Lim, H. Choi, I. S. Lim, S. B. Park, Y. S. Lee, S. K. Kim, *J. Phys. Chem. A* **2009**, 113, 10410.
- [21] a) J. C. Deaton, S. C. Switalski, D. Y. Kondakov, R. H. Young, T. D. Pawlik, D. J. Giesen, S. B. Harkins, A. J. M. Miller, S. F. Mickenberg, J. C. Peters, *J. Am. Chem. Soc.* **2010**, 132, 9499; b) B. Hupp, C. Schiller, C. Lenczyk, M. Stanoppi, K. Edkins, A. Lorbach, A. Steffen, *Inorg. Chem.* **2017**, 56, 8996; c) M. Z. Shafikov, A. F. Suleymanova, R. Czerwieniec, H. Yersin, *Inorg. Chem.* **2017**, 56, 13274; d) J. Nitsch, C. Kleeberg, R. Fröhlich, A. Steffen, *Dalton Trans.* **2015**, 44, 6944; e) V. W. W. Yam, E. C. C. Cheng, N. Zhu, *Angew. Chem.* **2001**, 40, 1763.
- [22] D. Sun, D.-F. Wang, F.-J. Liu, H.-J. Hao, N. Zhang, R.-B. Huang, L.-S. Zheng, *CrystEngComm* **2011**, 13, 2833.
- [23] M. Osawa, I. Kawata, R. Ishii, S. Igawa, M. Hashimoto, M. Hoshino, *J. Mater. Chem. C* **2013**, 1, 4375.
- [24] A. Barbieri, E. Bandini, F. Monti, V. K. Praveen, N. Armaroli, *Top. Curr. Chem.* **2016**, 374, 47.
- [25] a) P. Hohenberg, W. Kohn, *Phys. Rev.* **1964**, 136, B864-B871; b) W. Kohn, L. J. Sham, *Phys. Rev.* **1965**, 140, A1133.
- [26] K.-H. Low, C.-H. Li, V. A. L. Roy, S. S.-Y. Chui, S. L.-F. Chan, C.-M. Che, *Chem. Sci.* **2010**, 1, 515.
- [27] J. M. Forward, D. Bohmann, J. P. Fackler, R. J. Staples, *Inorg. Chem.* **1995**, 34, 6330.
- [28] a) V. W.-W. Yam, K. K.-W. Lo, *Chem. Soc. Rev.* **1999**, 28, 323; b) Q. Liu, M. Xie, X. Chang, Q. Gao, Y. Chen, W. Lu, *Chem. Commun.* **2018**, 54, 12844; c) R. Galassi, M. M. Ghimire, B. M. Otten, S. Ricci, R. N. McDougald, Jr., R. M. Almotawa, D. Alhmoud, J. F. Ivy, A.-M. M. Rawashdeh, V. N. Nesterov, E. W. Reinheimer, L. M. Daniels, A. Burini, M. A. Omary, *Proc. Natl. Acad. Sci. USA* **2017**, 114, E5042; d) I. Roppolo, E. Celasco, A. Fargues, A. Garcia, A. Revaux, G. Dantelle, F. Maroun, T. Gacoin, J.-P. Boilot, M. Sangermano, S. Perruchas, *J. Mater. Chem.* **2011**, 21, 19106.
- [29] A. Biswas, R. Bakthavatsalam, B. P. Mali, V. Bahadur, C. Biswas, S. S. K. Raavi, R. G. Gonnade, J. Kundu, *J. Mater. Chem. C* **2021**, 9, 348.

---

Manuscript received: February 2, 2022

Accepted manuscript online: February 15, 2022

Version of record online: March 4, 2022